OPTIMAL WINDOW DESIGN FOR W-OFDM

Khawar Hussain *Roberto López-Valcarce*

atlanTTic Research Center, University of Vigo, Spain. Email: {khawar,valcarce}@gts.uvigo.es

ABSTRACT

Windowing is an effective approach to reduce out-of-band radiation (OBR) in multicarrier systems in order to avoid adjacent channel interference. However, commonly used window functions are chosen in an *ad hoc* manner and fixed. We present an optimal window design for windowed-OFDM minimizing OBR within a given frequency region. The proposed technique is flexible in that it allows to specify the range of frequencies involved in the minimization and to apply spectral weighting. The optimal window can be computed offline.

***Index Terms*—** OFDM, windowing, out-of-band radiation, sidelobe suppression, inter-numerology interference, 5G

1. INTRODUCTION

The fifth-generation (5G) cellular communication framework is a stepping stone towards building a diverse system, as it will support a variety of user scenarios with diverse requirements. Enhanced-mobile broadband (eMBB), ultra-reliable and low latency communications (URLLC) and massive machine type communications (mMTC) are the three major types of services [1]. A robust waveform is required to cater to all these diverse requirements, and the Third Generation Partnership Project (3GPP) has agreed on the use of cyclic-prefix based orthogonal frequency division multiplexing (CP-OFDM) for the 5G new radio (5G-NR) interface [2]. OFDM is a mature technology with significant advantages: it is spectrally efficient, robust against frequency-selective channels, and well matched to multiple input-multiple output (MIMO) operation. It also has some drawbacks, e.g., large peak-to-average power ratio (PAPR), sensitivity to phase noise, and large spectrum sidelobes, causing high out-of-band radiation (OBR) which results in significant levels of adjacent channel interference.

Traditionally, the problem of OBR is mitigated by inserting large guard bands, which significantly degrades spectral efficiency. Many techniques have been proposed in the literature to tackle this problem. Constellation expansion [3] and multiple choice sequences [4] require transmitting side information, causing system overhead, whereas subcarrier weighting [5, 6] techniques are data dependent. Spectral precoding [7, 8, 9, 10, 11, 12] is another approach to reduce OBR, but it is not transparent and requires appropriate decoding at the receiver to compensate signal distortion. According to the latest 3GPP NR release [13], any operation performed on CP-OFDM at the transmitter side must be receiver agnostic [14]. Additionally, the aforementioned methods suffer in general from high complexity at both transmitter and receiver.

Another approach is to use *transmit windowing,* usually referred to as weighted overlap-add (WOLA) or windowed OFDM (W-OFDM) [15, 16], by which the standard rectangular pulse in CP-OFDM is replaced by a pulse with soft edges at both sides, resulting in much sharper sidelobe decay in the frequency domain. Moreover, W-OFDM is relatively less complex as compared to other OFDM-derived waveforms and has little or no peak-to-average power ratio (PAPR) overhead [17]. The price to pay in exchange for this improvement in terms of OBR is a reduction in spectral efficiency due to the newly introduced pulse edges, assuming that the length of the cyclic prefix stays the same; therefore, a tradeoff between spectral confinement and spectral efficiency appears.

A time-asymmetric per-subcarrier windowing scheme is proposed in [18] to tackle OBR and inter-symbol interference (ISI). Different window functions, e.g., raised cosine (RC), Hamming, Hanning, and Blackman were discussed in [19] along with the classical main lobe width / sidelobe level trade-off. The RC window is commonly used, as it offers a good compromise with straightforward implementation [20]. However, depending on the application, utilized bandwidth, active subcarrier set, etc., it may become useful to flexibly shape the power spectral density in order to focus on OBR at particular frequency regions. For example, depending on the particular spectral emission mask, one may want to sacrifice OBR performance for sufficiently far away frequencies in exchange for better performance near the transmitted spectrum edges. This cannot be done by using a single fixed window.

Motivated by the above consideration, we present a novel window design which is flexible enough to allow the aforementioned trade-off. The goal is to minimize the total OBR over a user-selectable frequency region; additionally, spectral weights may be included in the design in order to emphasize some frequency ranges over others. The proposed window can be computed offline, therefore the optimization process does not incur additional online complexity.

Supported by Agencia Estatal de Investigación (Spain) and the European Regional Development Fund (ERDF) under project WINTER (TEC2016-76409-C2-2-R, BES-2017-080305), and by Xunta de Galicia (Agrupación Estratéxica Consolidada de Galicia accreditation 2016-2019).

2. SIGNAL MODEL

Consider a CP-OFDM system with IFFT size N. Let $\mathcal{K} = \{k_1, k_2, \cdots k_K\}$ denote the set of indices of the K active subcarriers, and $x_k^{(m)}$ be the data modulated on the k-th subcarrier in the m-th symbol. The baseband samples of the multicarrier signal are given by

$$s[n] = \sum_{m=-\infty}^{\infty} \sum_{k \in \mathcal{K}} x_k^{(m)} h_{\mathrm{P}}[n - mL] e^{j\frac{2\pi}{N}k(n-mL)} \quad (1)$$

with L the hop size in samples, and $h_{\mathrm{P}}[n]$ the shaping pulse with Fourier transform $H_{\mathrm{P}}(e^{j\omega}) = \sum_n h_{\mathrm{P}}[n] e^{-j\omega n}$. In standard CP-OFDM (no windowing), $h_{\mathrm{P}}[n] = 1$ for $0 \leq n \leq L-1$, and zero otherwise; hence, there is no overlap between consecutive size-L blocks in (1), and a CP of $L - N$ samples is implicit. The analog baseband signal is

$$s(t) = \sum_{n=-\infty}^{\infty} s[n] h_{\mathrm{I}}(t - nT_s), \quad (2)$$

where T_s is the sampling interval, and $h_{\mathrm{I}}(t)$ the impulse response of the interpolation filter in the Digital-to-Analog Converter (DAC). Let us define $\phi_k(f) \triangleq H_{\mathrm{P}}^*(e^{j2\pi(f-k\Delta f)T_s})$, where $\Delta f = \frac{1}{NT_s}$ is the subcarrier spacing, and

$$\boldsymbol{\phi}(f) \triangleq [\ \phi_{k_1}(f) \quad \phi_{k_2}(f) \quad \cdots \quad \phi_{k_K}(f)\ ]^T. \quad (3)$$

Following steps analogous to those in [21], the power spectral density (PSD) of $s(t)$ can be shown[1] to be

$$S_s(f) = \frac{|H_{\mathrm{I}}(f)|^2}{LT_s} \boldsymbol{\phi}^H(f) \boldsymbol{A} \boldsymbol{\phi}(f), \quad (4)$$

where $\boldsymbol{A} \triangleq \mathbb{E}\{\boldsymbol{x}_m \boldsymbol{x}_m^H\}$, with $\boldsymbol{x}_m$ the vector of data symbols in the m-th block:

$$\boldsymbol{x}_m \triangleq [\ x_{k_1}^{(m)} \quad x_{k_2}^{(m)} \quad \cdots \quad x_{k_K}^{(m)}\ ]^T. \quad (5)$$

It is assumed that $\mathbb{E}\{\boldsymbol{x}_m \boldsymbol{x}_m^H\}$ is independent of m.

With the introduction of windowing, the length of the pulse $h_{\mathrm{P}}[n]$ is extended Q samples with respect to standard CP-OFDM. Thus, $h_{\mathrm{P}}[n]$ is nonzero only for $n \in \{0, 1, \ldots, L + Q - 1\}$, and there is an overlap of Q samples between consecutive blocks in (1). In particular, whereas the central samples are still fixed to 1, i.e., $h_{\mathrm{P}}[n] = 1$ for $Q \leq n \leq L - 1$, the edge samples $h_{\mathrm{P}}[0]$,…,$h_{\mathrm{P}}[Q-1]$ and $h_{\mathrm{P}}[L]$,…,$h_{\mathrm{P}}[L+Q-1]$ are allowed to take different values. The gradual transition from 0 to 1 of these edge samples results in a sharper PSD [15]. On the other hand, due to the Q-sample overlap, the effective CP has been reduced to $L - N - Q$ samples; therefore, for a given effective CP length (determined by the expected channel delay spread), windowing results in a reduction of spectral efficiency by a factor $\frac{N}{L+Q}$.

[1]The detailed derivation of (4) is skipped due to space constraints.

3. OPTIMAL WINDOW DESIGN

For a given Q, we seek to optimize the free coefficients in the pulse $h_{\mathrm{P}}[n]$ in terms of OBR. Our cost function is given by

$$\mathcal{P} = \int_{-\infty}^{\infty} W(f) S_s(f) \mathrm{d}f, \quad (6)$$

where $W(f) \geq 0$ is a nonnegative spectral weighting function, giving emphasis to those frequency ranges over which OBR reduction is important. To proceed, note that $\boldsymbol{\phi}(f)$ in (3) can be rewritten as $\boldsymbol{\phi}(f) = \boldsymbol{M}(f)\boldsymbol{h}^*$, where $\boldsymbol{h} \in \mathbb{C}^{L+Q}$ comprises the pulse samples:

$$\boldsymbol{h} \triangleq [\ h[0] \quad h[1] \quad \cdots \quad h[L+Q-1]\ ]^T, \quad (7)$$

and $\boldsymbol{M}(f) \in \mathbb{C}^{K \times (L+Q)}$ is given entrywise by

$$[\boldsymbol{M}(f)]_{pq} = e^{j2\pi(q-1)(f-k_p\Delta f)}, \begin{cases} p &= 1, \ldots, K, \\ q &= 1, \ldots, L+Q. \end{cases} \quad (8)$$

Thus, the PSD $S_s(f)$ in (4) can be rewritten in terms of $\boldsymbol{h}$ as

$$S_s(f) = \frac{|H_I(f)|^2}{LT_s} \boldsymbol{h}^T \boldsymbol{M}^H(f) \boldsymbol{A} \boldsymbol{M}(f) \boldsymbol{h}^*, \quad (9)$$

so that the spectrally weighted power in (6) becomes $\mathcal{P} = \boldsymbol{h}^H \boldsymbol{Z} \boldsymbol{h}$, where the matrix $\boldsymbol{Z} \in \mathbb{C}^{(L+Q)\times(L+Q)}$ is given by

$$\boldsymbol{Z} \triangleq \frac{1}{LT_s} \int_{-\infty}^{\infty} W(f) |H_{\mathrm{I}}(f)|^2 \boldsymbol{M}^T(f) \boldsymbol{A}^* \boldsymbol{M}^*(f) \mathrm{d}f, \quad (10)$$

which is Hermitian positive (semi)definite. Then the window design problem for the minimization of $\mathcal{P}$ becomes

$$\min_{\boldsymbol{h}} \boldsymbol{h}^H \boldsymbol{Z} \boldsymbol{h} \quad \text{s. to} \quad \boldsymbol{S}^H \boldsymbol{h} = \boldsymbol{1}, \quad (11)$$

where $\boldsymbol{S} \in \mathbb{C}^{(L+Q)\times(L-Q)}$ comprises columns $Q+1$ through L of the identity matrix $\boldsymbol{I}_{L+Q}$, and $\boldsymbol{1} \in \mathbb{C}^{L-Q}$ is the all-ones vector. The solution of this convex minimization problem can be readily found in closed form.

4. RESULTS AND DISCUSSION

The proposed window design provides flexibility to achieve various levels of OBR reduction in different frequency regions, determined by the chosen spectral weighting function $W(f)$, according to system requirements. Let us consider a CP-OFDM system with subcarrier spacing $\Delta f = 15$ kHz and 7 % CP overhead, as in LTE/5G. It is assumed that $\boldsymbol{A} = \boldsymbol{I}_K$, i.e., all active subcarriers are mutually uncorrelated and with the same power, and that $H_{\mathrm{I}}(f)$ is an ideal lowpass filter with $H_{\mathrm{I}}(f) = 1$ for $|f| \leq \frac{1}{2T_s}$ and zero otherwise. The IFFT size is $N = 1024$. Fig. 1 shows the PSD of the proposed optimum window design (OW-OFDM), along with non-windowed CP-OFDM and raised cosine W-OFDM (RCW-OFDM) for a user

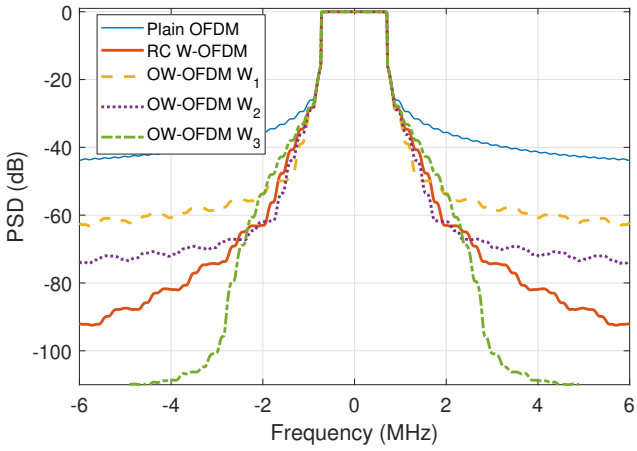

Fig. 1. PSD of OW-OFDM, RC W-OFDM and CP-OFDM for $Q = 1/4$ CP and different spectral weighting functions.

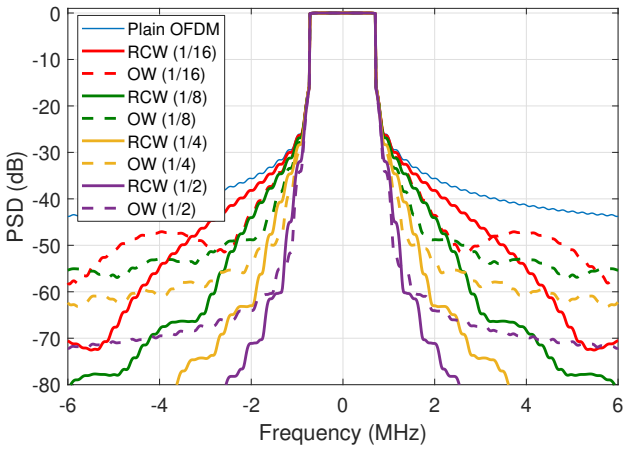

Fig. 2. PSD of OW-OFDM (dashed), RCW-OFDM (solid) and CP-OFDM (thin solid) for different window overhead values (expressed as a fraction of the CP length).

with 96 active subcarriers (i.e., 8 resource blocks (RBs) of 12 subcarriers each); the size of the window edge Q is set to $1/4$ of the CP for both OW-OFDM and RCW-OFDM.

Three different weighting functions were considered:

$$W_1(f) = 1, \quad 1.02 \text{ MHz} \leq |f| \leq 6.5 \text{ MHz}, \quad (12)$$

$$W_2(f) = 1, \quad 1.47 \text{ MHz} \leq |f| \leq 6.5 \text{ MHz}, \quad (13)$$

$$W_3(f) = 1, \quad 2.82 \text{ MHz} \leq |f| \leq 6.5 \text{ MHz}, \quad (14)$$

and $W_i(f) = 0$ elsewhere. The optimum window based on W_1 provides more OBR reduction in the vicinity of the transmitted spectrum edges than the RC window, at the expense of less reduction for $|f| \geq 1.65$ MHz (at which the PSD is already 50 dB below the passband value). With W_2, the optimal window results in a PSD below that for the RC window for $|f| \leq 2$ MHz, at which 60 dB w.r.t. the passband have been achieved. However, the PSD for W_1 is below that for W_2 for $|f| \leq 1.48$ MHz. Finally, with W_3 no weight is given to nearby frequencies, and therefore very low PSD values can be attained for distant frequencies in exchange for spectral regrowth closer to the spetrum edges. This illustrates how the proposed optimal window design is flexible enough to accommodate different requirements.

The window edge size Q is another critical factor, which directly impacts the performance of the window. Larger values of Q provide better OBR reduction at the cost of reduced effective CP, as discussed in Sec. 2. Thus, on one hand, Q should be small enough to leave a sufficiently long CP to combat multipath, and on the other, it should be large enough to achieve the required OBR reduction. To illustrate this, Fig. 2 shows the PSD obtained in the same setting as that of Fig. 1 ($\Delta f = 15$ kHz, 7% CP, $N = 1024$, $K = 96$) with an RC window and with the proposed design using weighting function $W_2(f)$ from (13), for different values of Q. For small window overhead (Q = 1/16 CP), the PSD of RC W-OFDM decays very slowly and gradually, and the proposed design provides significant improvement for $|f| \leq 3.3$ MHz. This trend continues for increasing values of Q, with the frequency at which the PSDs of RCW-OFDM and OW-OFDM cross getting closer to the spectrum edge. We note that OW-OFDM can be further optimized using a different weighting function to achieve OBR requirements in a particular frequency range.

To quantify performance in a specific interference scenario, consider a setting with two asynchronous users, each of which is assigned 8 RBs (96 subcarriers), and there is no guard band between these two transmissions. We assume $\Delta f = 15$ kHz, 7% CP, $N = 1024$ as before, and $Q = 1/4$ CP, so each user can use the windows considered in the setting of Fig. 1. Fig. 3 shows the signal-to-interference ratio (SIR), defined as the ratio of the PSDs of the signal and the interference when both suffer the same frequency-flat attenuation, for different window choices. It is seen that the proposed design provides better SIR than RC W-OFDM and plain CP-OFDM near edge subcarriers. The use of weight function W_1 is likely more meaningful in this setting than W_2, since the latter outperforms the former only for very high values of SIR (> 50 dB), a regime in which channel noise, and not interference, is likely to be the limiting factor.

5G systems may use different numerologies (i.e., different subcarrier spacings), for different scenarios [22], e.g., using larger subcarrier spacing (hence shorter symbol duration) for low latency or enhanced robustness to phase noise and Doppler spread, and smaller subcarrier spacing (hence longer symbol and CP duration) for settings with long delay spreads, as in large cells. Different services can be frequency-multiplexed by assigning them different numerologies in different subbands [23]. However, although within a given numerology subcarriers are mutually orthogonal, subcarri-

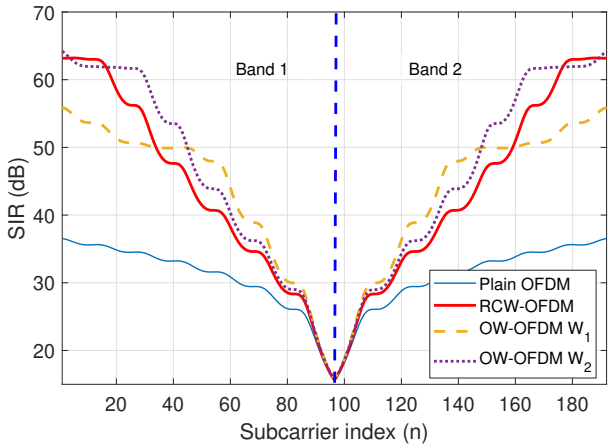

Fig. 3. Signal-to-Interference Ratio for two asynchronous users with $\Delta f = 15$ kHz. $Q = 1/4$ CP.

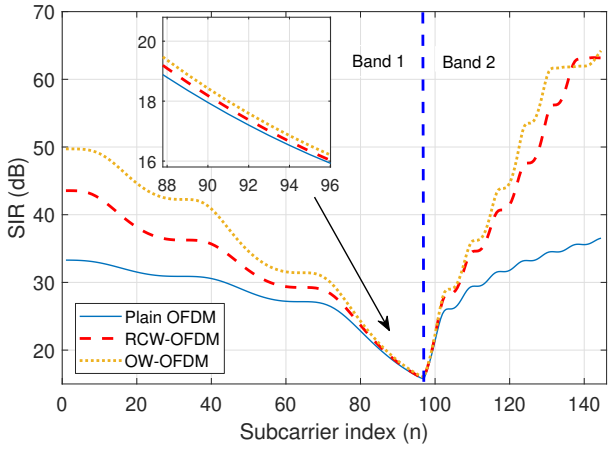

Fig. 4. Signal-to-Interference Ratio for two adjacent numerologies: $\Delta f_1 = 15$ kHz, $\Delta f_2 = 30$ kHz. $Q = 1/4$ CP.

ers with different numerologies may cause interference to each other, especially if they are close in frequency. This effect, known as inter-numerology interference (INI), may significantly degrade performance [22, 23].

We consider next a scenario in which two adjacent (i.e., no guard band) frequency subbands accommodate different numerologies: band 1 with subcarrier spacing $\Delta f_1 = 15$ kHz, and band 2 with $\Delta f_2 = 30$ kHz. Band 1 transmits 8 RBs whereas band 2 is using 4 RBs, so that the occupied bandwidth is the same for both bands (1.44 MHz). The CP overhead is set to 7% and the window edge size Q is $1/4$ CP for both numerologies. In the design of the optimum window for band 1, the weighting function was taken as $W(f) = 1$ for frequencies farther than 1.47 MHz from the center frequency, and zero otherwise; whereas for band 2, the corresponding

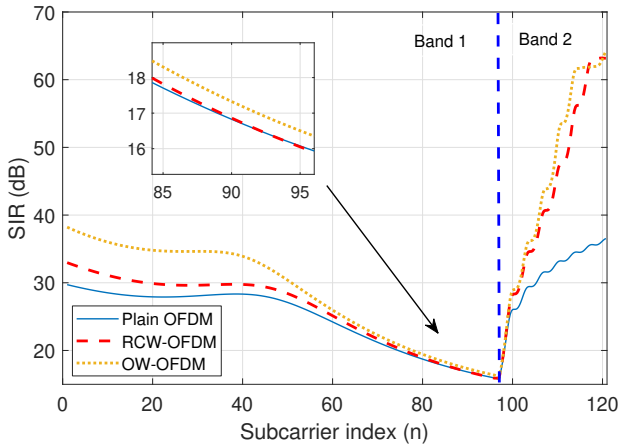

Fig. 5. Signal-to-Interference Ratio for two adjacent numerologies: $\Delta f_1 = 15$ kHz, $\Delta f_2 = 60$ kHz. $Q = 1/4$ CP.

value was taken as 1.32 MHz. Fig. 4 shows the corresponding SIR values. Band 1 suffers from more interference from band 2, as the latter has wider subcarriers with sidelobes decreasing more slowly. The proposed design provides significant improvement in SIR over both subbands as compared to RCW-OFDM, for the same window overhead.

Furthermore, if band 2 uses a wider subcarrier spacing, it will cause higher interference to the adjacent band 1. Fig. 5 shows the results in such scenario, where band 2 is now using a subcarrier spacing of $\Delta f_2 = 60$ kHz and transmits 2 RBs; whereas the parameters for band 1 were the same as in the previous case. The spectral weighting for band 2 was now taken as $W(f) = 1$ for frequencies farther than 0.72 MHz from its center frequency and zero otherwise. It can be seen that the SIR for band 1 is significantly lower than in the previous case, highlighting the benefits of an optimized window design.

5. CONCLUSION

Windowing at the transmit side is an effective way to reduce out-of-band radiation, with the benefit of having low implementation complexity and being transparent to the receiver. A novel window design for multicarrier systems has been presented, focusing on the reduction of out-of-band radiation. The proposed design provides the flexibility to minimize the OBR in a given frequency region which is user-selectable, with the possibility of assigning different weights to different subregions. This tradeoff is particularly appealing for mitigating internumerology interference in 5G systems. Since the optimized window is computed offline, the online computational complexity is the same as that for other windowing techniques.

6. REFERENCES

[1] E. Dahlman, S. Parkvall, and J. Skold, *5G NR: The Next Generation Wireless Access Technology*, Academic Press, London, UK, 2018.

[2] Group Radio Access Network, "TS38.211: NR; Physical channels and modulation (Release 15)," `https://portal.3gpp.org/desktopmodules/Specifications/SpecificationDetails.aspx?specificationId=3213`, Mar. 2018.

[3] S. Pagadarai, R. Rajbanshi, A. M. Wyglinski, and G. J. Minden, "Sidelobe suppression for OFDM-based cognitive radios using constellation expansion," in *IEEE Wireless Commun. Netw. Conf.*, 2008, pp. 888–893.

[4] I. Cosovic and V. Janardhanam, "Sidelobe suppression in ofdm systems," in *Multi-Carrier Spread-Spectrum*, Khaled Fazel and Stefan Kaiser, Eds., Dordrecht, 2006, pp. 473–482, Springer Netherlands.

[5] I. Cosovic, S. Brandes, and M. Schnell, "Subcarrier weighting: a method for sidelobe suppression in OFDM systems," *IEEE Commun. Lett.*, vol. 10, no. 6, pp. 444–446, Jun. 2006.

[6] R. Kumar and A. Tyagi, "Extended subcarrier weighting for sidelobe suppression in OFDM based cognitive radio," *Wireless Pers. Commun.*, vol. 87, no. 3, pp. 779–796, Apr. 2016.

[7] C.-D. Chung, "Correlatively coded OFDM," *IEEE Trans. Wireless Commun.*, vol. 5, no. 8, pp. 2044–2049, Aug. 2006.

[8] C. Chung, "Spectrally precoded OFDM," *IEEE Trans. Commun.*, vol. 54, no. 12, pp. 2173–2185, Dec 2006.

[9] K. Hussain, A. Lojo, and R. López-Valcarce, "Flexible spectral precoding for sidelobe suppression in ofdm systems," in *ICASSP 2019 - 2019 IEEE International Conference on Acoustics, Speech and Signal Processing (ICASSP)*, May 2019, pp. 4789–4793.

[10] K. Hussain and R. López-Valcarce, "OFDM spectral precoding with per-subcarrier distortion constraints," in *2019 27th European Signal Processing Conference (EUSIPCO)*, 2019, accepted.

[11] J. van de Beek and F. Berggren, "N-continuous OFDM," *IEEE Commun. Lett.*, vol. 13, no. 1, pp. 1–3, Jan. 2009.

[12] J. van de Beek, "Sculpting the multicarrier spectrum: a novel projection precoder," *IEEE Commun. Lett.*, vol. 13, no. 12, pp. 881–883, Dec. 2009.

[13] J. G. Andrews, S. Buzzi, W. Choi, S. V. Hanly, A. Lozano, A. C. K. Soong, and J. C. Zhang, "What will 5G be?," *IEEE J. Sel. Areas Commun.*, vol. 32, no. 6, pp. 1065–1082, June 2014.

[14] A. Zaidi, F. Athley, J. Medbo, U. Gustavsson, G. Durisi, and X. Chen, *5G Physical Layer: Principles, Models and Technology Components*, Academic Press, London, UK, 2018.

[15] R. Zayani, Y. Medjahdi, H. Shaiek, and D. Roviras, "WOLA-OFDM: A potential candidate for asynchronous 5G," in *2016 IEEE Global Commun. Workshops*, Dec 2016, pp. 1–5.

[16] A. A. Zaidi, R. Baldemair, H. Tullberg, H. Bjorkegren, L. Sundstrom, J. Medbo, C. Kilinc, and I. Da Silva, "Waveform and numerology to support 5G services and requirements," *IEEE Commun. Mag.*, vol. 54, no. 11, pp. 90–98, November 2016.

[17] S. Lien, S. Shieh, Y. Huang, B. Su, Y. Hsu, and H. Wei, "5G new radio: Waveform, frame structure, multiple access, and initial access," *IEEE Commun. Mag.*, vol. 55, no. 6, pp. 64–71, June 2017.

[18] E. Guvenkaya, E. Bala, R. Yang, and H. Arslan, "Time-asymmetric and subcarrier-specific pulse shaping in OFDM-based waveforms," *IEEE Trans. Veh. Technol.*, vol. 64, no. 11, pp. 5070–5082, Nov 2015.

[19] B. Farhang-Boroujeny, "OFDM versus filter bank multicarrier," *IEEE Signal Process. Mag.*, vol. 28, no. 3, pp. 92–112, May 2011.

[20] Document R1-162199, "Waveform candidates," Qualcomm Inc., Busan, South Korea, Apr. 2016.

[21] T. van Waterschoot, V. Le Nir, J. Duplicy, and M. Moonen, "Analytical expressions for the power spectral density of CP-OFDM and ZP-OFDM signals," *IEEE Signal Process. Lett.*, vol. 17, no. 4, pp. 371–374, Apr. 2010.

[22] P. Guan *et al.*, "5G field trials: OFDM-based waveforms and mixed numerologies," *IEEE J. Sel. Areas Commun.*, vol. 35, no. 6, pp. 1234–1243, Jun 2017.

[23] X. Zhang, L. Zhang, P. Xiao, D. Ma, J. Wei, and Y. Xin, "Mixed numerologies interference analysis and inter-numerology interference cancellation for windowed OFDM systems," *IEEE Trans. Veh. Technol.*, vol. 67, no. 8, pp. 7047–7061, Aug 2018.